Corrections

BIOCHEMISTRY. For the article "HuR binding to cytoplasmic mRNA is perturbed by heat shock," by Imed-Eddine Gallouzi, Christopher M. Brennan, Myrna G. Stenberg, Maurice S. Swanson, Ashley Eversole, Nancy Maizels, and Joan A. Steitz, which appeared in number 7, March 28, 2000, of *Proc. Natl. Acad. Sci. USA* (**97,** 3073–3078), the authors note the following regarding Fig. 2. Attempts to repeat *in situ* hybridization experiments comparing the localization of poly(A)$^+$ RNA in HeLa cells before and after heat shock have revealed that the differences are not as dramatic as those seen in panels 13 and 14. Rather, the nearly complete absence of poly(A)$^+$ RNA from the nuclear region is observed only in metaphase cells, which were mistakenly selected for display in panel 13. In nondividing cells at 37°C, a significant poly(A)$^+$ signal is usually seen in the nucleus in addition to that in the cytoplasm. The major conclusions of the paper remain unchanged.

www.pnas.org/cgi/doi/10.1073/pnas.0337430100

BIOCHEMISTRY. For the article "Structure and function from the circadian clock protein KaiA of *Synechococcus elongatus*: A potential clock input mechanism," by Stanly B. Williams, Ioannis Vakonakis, Susan S. Golden, and Andy C. LiWang, which appeared in number 24, November 26, 2002, of *Proc. Natl. Acad. Sci. USA* (**99,** 15357–15362; First Published November 15, 2002; 10.1073/pnas.232517099), on page 15358, left column, third full paragraph, lines 9 and 15, the terms H^{γ} and H^{Δ} appeared incorrectly due to printer's errors. In line 9, H^{γ} should read H^{β} and, in line 15, H^{Δ} should read H^{δ}.

www.pnas.org/cgi/doi/10.1073/pnas.0337360100

BIOCHEMISTRY. For the article "Overexpression, purification, and site-directed spin labeling of the Nramp metal transporter from *Mycobacterium leprae*," by Ian Reeve, David Hummell, Nathan Nelson, and John Voss, which appeared in number 13, June 25, 2002, of *Proc. Natl. Acad. Sci. USA* (**99,** 8608–8613; First Published June 19, 2002; 10.1073/pnas.142287699), the author name David Hummell should have been spelled David Hummel. The online version has been corrected. The corrected author line appears below.

Ian Reeve, David Hummel, Nathan Nelson, and John Voss

www.pnas.org/cgi/doi/10.1073/pnas.0337129100

MEDICAL SCIENCES. For the article "Inflammatory mediators are induced by dietary glycotoxins, a major risk factor for diabetic angiopathy," by Helen Vlassara, Weijing Cai, Jill Crandall, Teresia Goldberg, Robert Oberstein, Veronique Dardaine, Melpomeni Peppa, and Elliot J. Rayfield, which appeared in number 24, November 26, 2002, of *Proc. Natl. Acad. Sci. USA* (**99,** 15596–15601; First Published November 12, 2002; 10.1073/pnas.242407999), the authors note that the following statement was omitted from the Acknowledgments. "The research presented in the paper was also supported by Grant MO1-RR-00071 from the National Center for Research Resources (NCRR), awarded to the General Clinical Research Center at Mount Sinai School of Medicine."

www.pnas.org/cgi/doi/10.1073/pnas.0337131100

NEUROSCIENCE. For the article "Stepwise contribution of each subunit to the cooperative activation of BK channels by Ca^{2+}," by Xiaowei Niu and Karl L. Magleby, which appeared in number 17, August 20, 2002, of *Proc. Natl. Acad. Sci. USA* (**99,** 11441–11446; First Published August 2, 2002; 10.1073/pnas.172254699), Eq. **1** on page 11444 appeared incorrectly. The correct equation appears below.

$$Po = \frac{P_{max}}{1 + (K_d/Ca_i^{2+})^n} \qquad [1]$$

www.pnas.org/cgi/doi/10.1073/pnas.0337132100

MICROBIOLOGY. For the article "The total influenza vaccine failure of 1947 revisited: Major intrasubtypic antigenic change can explain failure of vaccine in a post-World War II epidemic," by Edwin D. Kilbourne, Catherine Smith, Ian Brett, Barbara A. Pokorny, Bert Johansson, and Nancy Cox, which appeared in number 16, August 6, 2002, of *Proc. Natl. Acad. Sci. USA* (**99,** 10748–10752; First Published July 22, 2002; 10.1073/pnas.162366899), in Table 7, three entries in the first two data columns appeared incorrectly. The corrected table appears below. The sequences submitted to GenBank are correct. In addition, on page 10751, left column, line 5, "7 of 11 antigenic sites" should read "8 of 11 antigenic sites." These errors do not affect the interpretations and conclusions of the paper.

Table 7. Antigenic site changes in the HA gene

	Antigenic site												
	Sa				Sb			Ca1		Ca2		Cb	
	163	165	166	129	192	196	197	173	273	145	225	78	81
1943–1947													
Weiss/43	Y	R	N		Q	Q		A	S	R	D	L	E
Marton/43	N	N	N		Q	Q		G	S	S	G	Q	E
FM/1/47	K	S	K		K	R		E	P	S	G	L	K
Rhodes/47	N	S	K		R	R		E	S	S	G	L	K
1977–1986													
USSR/90/77				K	K	R	T				G		
India/6263/80				K	K	R	T				D		
Chile/1/83				K	K	R	T				N		
Taiwan/1/86				N	R	H	A				G		

www.pnas.org/cgi/doi/10.1073/pnas.0337361100.

Structure and function from the circadian clock protein KaiA of *Synechococcus elongatus*: A potential clock input mechanism

Stanly B. Williams*†, Ioannis Vakonakis†‡, Susan S. Golden*§, and Andy C. LiWang‡¶

Departments of *Biology and ‡Biochemistry and Biophysics, Texas A&M University, College Station, TX 77843

Edited by Robert Haselkorn, University of Chicago, Chicago, IL, and approved September 17, 2002 (received for review August 26, 2002)

In the cyanobacterium *Synechococcus elongatus* (PCC 7942) the proteins KaiA, KaiB, and KaiC are required for circadian clock function. We deduced a circadian clock function for KaiA from a combination of biochemical and structural data. Both KaiA and its isolated carboxyl-terminal domain (KaiA180C) stimulated KaiC autophosphorylation and facilitated attenuation of KaiC autophosphorylation by KaiB. An amino-terminal domain (KaiA135N) had no function in the autophosphorylation assay. NMR structure determination showed that KaiA135N is a pseudo-receiver domain. We propose that this pseudo-receiver is a timing input-device that regulates KaiA stimulation of KaiC autophosphorylation, which in turn is essential for circadian timekeeping.

Circadian clocks among disparate groups of organisms share functional properties, but the proteins identified at their central cores lack sequence similarity beyond the PAS domains present in some, and there are no structural data available to reveal possible shared functions (1). In the cyanobacterium *Synechococcus elongatus* (PCC 7942), a model organism for prokaryotic circadian biology, the *kai* locus consists of three genes required for circadian clock function (2). None of the Kai proteins (KaiA, KaiB, or KaiC) shares sequence similarity with any eukaryotic clock protein (1, 3), even though the fundamental properties of cyanobacterial circadian rhythmicity (near 24-h free-running period, phase resetting by light, and a temperature compensation mechanism) are equivalent to those first established for numerous eukaryotic organisms including *Neurospora crassa*, *Arabidopsis thaliana*, and *Drosophila melanogaster* (3). We report here biochemical and structural data for KaiA, which together sanction a model in which the amino-terminal pseudo-receiver is a timing-input device that regulates carboxyl-terminal KaiA stimulation of KaiC autophosphorylation, which in turn is essential for circadian timekeeping.

The *kai* genes are ubiquitous among cyanobacteria, with probable *kaiC* sequence identified in forty phylogenetically diverse species (4). Accordingly, all six sequenced and annotated cyanobacterial genomes contain two contiguous ORFs with apparent homology to the *S. elongatus kaiB* and *kaiC* genes (annotated genome sequences for *Synechocystis* sp. strain PCC 6803 and *Anabaena* sp. strain PCC 7120 are available at www.kazusa.or.jp/cyano/ and, for *Prochlorococcus marinus* MED4, *Prochlorococcus marinus* MIT9313, *Synechococcus* sp. strain WH8102, and *Nostoc punctiforme* at www.jgi.doe.gov/JGI_home.html). Across these species *kaiA* is the most sequence-diversified of the *kai* genes, as only four are identifiable via sequence comparisons. Curiously, the *Synechocystis* sp. strain PCC 6803 genome, which contains multiple *kaiB* and *kaiC* genes, has only one *kaiA* gene. Apparent homologues of *kaiB* and *kaiC* are found among noncyanobacterial eubacteria and the archaea. However, the *kaiA* gene appears confined within the cyanobacteria, which are the only prokaryotes with demonstrated circadian rhythms.

S. elongatus Kai proteins form oligomeric complexes *in vitro* in all possible combinations (5). *In vivo* data support formation of a higher-order complex that contains, at minimum, multiple protomers of each of the three Kai proteins, and likely includes the SasA protein kinase. In addition, both KaiB and KaiC protein levels, but not those of KaiA, display circadian cycles under free-running, constant-light conditions (5, 6). In functional terms, we know that point mutations in *kaiC*, which alter ATP binding and autokinase activities of KaiC, disrupt circadian rhythms of gene expression (7, 8). Cycles of KaiC phosphorylation also occur in a circadian time frame (9). These observations led us to ask how Kai protein interactions might affect the rate of KaiC autophosphorylation.

Materials and Methods

Cloning and Protein Purification. The genes encoding KaiB, KaiA, KaiA135N, KaiA189N, and KaiA180C were cloned into the pET32a+ vector (Novagen) and subsequently overexpressed in *Escherichia coli* BL21(DE3) (Novagen). Genes encoding KaiC and KaiA were cloned into plasmid pQE32 (Qiagen, Valencia, CA) and subsequently overexpressed in *E. coli* M15 (Qiagen). This latter 6His-tagged KaiA was used only in the autophosphorylation assays. All other data were collected by using the pET32a+-derived KaiA protein. The QuikChange method from Stratagene was used to create site-specific mutations. DNA from relevant clones was then sequenced for verification (Gene Technologies Lab, Texas A&M University). For NMR sample preparation, bacteria were grown at 37°C in a minimal medium containing $^{15}NH_4Cl$ as the only nitrogen source, and either $^{13}C_6$-glucose or unlabeled glucose as carbon source. Adding isopropyl β-D-thiogalactosepytanoside to 1 mM induced overproduction of the relevant protein. Cells were harvested after 5 h. Cell pellets containing KaiA, KaiA189N, and KaiA180C were resuspended in aqueous 20 mM Tris·HCl at pH 7.0 with 10 mM NaCl. For KaiA135N 50 mM NaCl was used. For KaiC, 6His-KaiA, and KaiB overproduction the cells were harvested 3.5 h after induction. Cell pellets were resuspended in aqueous 50 mM Tris·HCl at pH 7.5 with 300 mM KCl, 10 mM $MgCl_2$, and 1 mM 2-mercaptoethanol. The solubility of KaiC was increased by also adding 1 mM ATP to the resuspension solution. Cell suspensions were passed twice through a French Press cell and the lysates clarified by centrifugation at 20,000 $\times$ *g* for 30 min. Tagged proteins were purified from the supernatant fraction on a Ni-charged chelating column and, if appropriate, dialyzed against the recommended enterokinase cleavage buffer (Novagen). After enterokinase cleavage (Novagen), the thioredoxin tag was separated from Kai protein by using a Ni-charged chelating column. All proteins were analyzed for purity by using

This paper was submitted directly (Track II) to the PNAS office.

Data deposition: The crystal structures and coordinates reported in this paper have been deposited in the Protein Data Bank, www.rcsb.org (PBD ID codes 1M2E and 1M2F).

†S.B.W. and I.V. contributed equally to this work.

§To whom correspondence regarding circadian aspects should be addressed. E-mail: sgolden@tamu.edu.

¶To whom correspondence regarding structural aspects should be addressed. E-mail: andy-liwang@tamu.edu.

BIOCHEMISTRY

SDS/PAGE and dialyzed to an appropriate final buffer, either for NMR spectroscopy or autophosphorylation assay.

Autophosphorylation Assays. Autophosphorylation assays were run at 25°C. KaiC protein was at 1 μM in aqueous buffer containing 25 mM Tris·HCl, 200 mM KCl, 1 mM 2-mercaptoethanol and 5 mM $MgCl_2$ at pH 7.5. To ensure initial velocity measurements, we did experiments over a range of constituent concentrations and established that 1 mM ATP, 3 μM KaiA, and 3 μM KaiB were saturating for KaiC autophosphorylation rate determinations (data not shown). The negative effect of KaiB on the KaiC-KaiA complex was also greatest with 1 mM ATP and 3 μM KaiB (data not shown). The addition of BSA (New England Biolabs), thioredoxin (Novagen plasmid pET32a+), SasA (10), or CikA (11) protein had no effect on KaiC autophosphorylation rates under any of our assay conditions (data not shown). The two independent KaiA domains were also added at 3 μM as determined by additional experiments as conducted for the full-length protein. Relevant proteins were mixed for at least 2 min before the assays were started by the addition of radiolabeled ATP. Time "zero" samples were taken immediately after this latter addition. Samples, taken at the indicated times, were thermally denatured and run on SDS/PAGE gels. Phosphorimages of dried gels were used to quantify the amount of $^{32}PO_3^{2-}$ incorporated into KaiC. Numerical values representing the percentage of the highest level of incorporation for a given experiment were determined. These values were averaged for each reaction condition (protein components) and plotted as a linear function of time. Relative rates are the slopes of the calculated regression lines.

Limited Proteolysis Assay. We added 0.5 μg of trypsin (Promega) to 100 μl of 0.1 mM KaiA in aqueous buffer containing 50 mM Tris·HCl, pH 7.6 at 25°C. Samples were taken at the indicated timepoints, thermally denatured and run on an SDS/PAGE gel. Apparent molecular weight and amino-terminal sequencing (Protein Chemistry Laboratory, Texas A&M University) were used to identify the three major species.

NMR Spectroscopy. The solution conditions and chemical shift assignments of KaiA135N have been reported earlier (12). Additionally, chemical shift assignments for aromatic groups were identified by interpretation of the NOESY spectra. The oxidation states of the cysteine residues were determined as reduced by their $^{13}C^{\beta}$ chemical shifts. The isomerization state of all proline residues was determined (13) as *trans* except Pro-130, which was in the *cis* configuration. Stereospecific assignments of methylene H^{γ} protons as well as χ_1 angle determinations (60°, −60°, 180°) were preformed by using HNHB (14) and HACAHB (15) experiments. Additional χ_1 angles for valine, isoleucine, and threonine residues, as well as stereospecific assignments of valine H^{γ} methyl groups were obtained by determining long range ^{15}N and $^{13}C'$ J-couplings to side chain methyl groups (16, 17). Because of limited chemical shift dispersion of leucine H^{Δ} and isoleucine $H^{\delta 1}$ methyl groups we were able to determine only 1 χ_2 angle out of 22 total using a ^{13}C-^{13}C J-coupling experiment (18). Stereospecific assignments of leucine H^{δ} methyl groups and proline methylene protons were found by interpreting the NOESY spectra. φ and ψ backbone angles were restrained by TALOS (19). ^1H–^1H NOE distance restraints were obtained by using ^{13}C–^{15}N edited and ^{13}C–^{13}C edited 4D NOESY spectra (20). Backbone ^{15}N relaxation measurements (T_1, T_2, and NOE) were performed and analyzed as described earlier (21).

Structure Calculations. ^1H–^1H distances were grouped into four ranges depending on the NOESY cross-peak intensity. The lower distance bound was fixed to 1.8 Å. The upper distance bound was 2.7 Å for strong NOESY cross-peaks (2.9 Å for cross-peaks involving amide protons), 3.3 Å for medium NOESY cross-peaks (3.5 Å for cross-peaks involving amide protons), 5.0 Å for weak NOESY cross-peaks, and 6.0 for very weak NOESY cross-peaks. The upper distance bound was increased by 0.5 Å for the NOESY cross-peaks involving methyl groups. A distance geometry simulated annealing protocol was used under the program X-PLOR (22) to calculate structures of KaiA135N. During the refinement and minimization stages, a conformational database potential (23, 24) was applied in addition to the usual potentials.

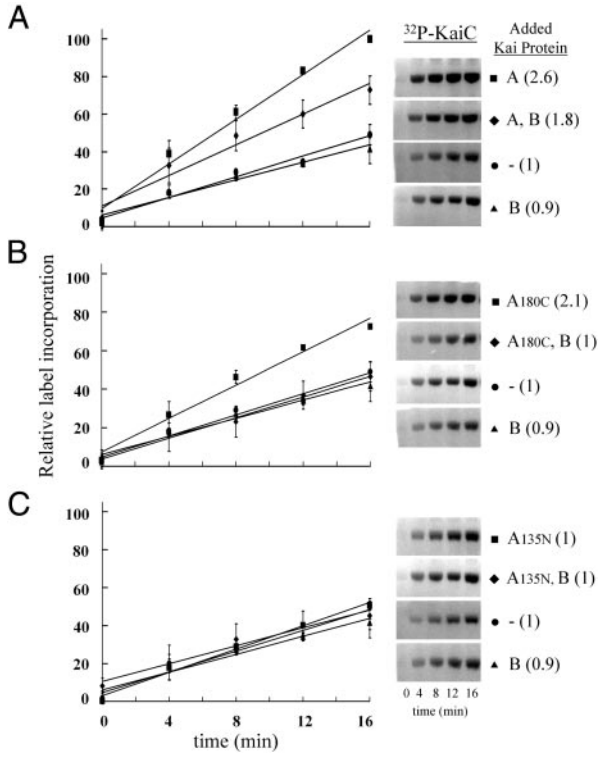

Fig. 1. Influence of Kai proteins on the autophosphorylation rate of KaiC. (*A*) Assays were run under initial rate conditions as described (see *Materials and Methods*). The graph illustrates the time course of KaiC autophosphorylation with ATP in the presence of KaiA, KaiA and KaiB, no additional protein, and KaiB. All time points are the average of four independent experiments, including the one represented by the gel images. Error bars indicate standard deviation from the mean ($n = 4$). Relative rates calculated from the line slopes are indicated parenthetically. (*B*) As above but the KaiA180C domain was substituted for KaiA in each assay. (*C*) As above but the Kai135N domain was substituted for KaiA in each assay.

Results

Relative KaiC Autophosphorylation Rates. The *in vitro* rate of KaiC autophosphorylation provided an assay for examining Kai protein functional interactions. Purified KaiC was incubated with [γ-^{32}P] adenosine 5′-triphosphate alone and also in combination with the KaiA and KaiB proteins. Initial rate conditions were established as described in *Materials and Methods*. Surprisingly, the rate of KaiC autophosphorylation was unaltered by the addition of KaiB even though these two proteins are known to interact (5) (Fig. 1*A*). Addition of KaiA to the assay increased the KaiC autophosphorylation rate ≈2.5-fold (Fig. 1*A*). In assays that included all three Kai proteins the rate of autophosphorylation was increased relative to KaiC alone, yet decreased relative to the KaiA–KaiC protein combination (Fig. 1*A*). Thus, KaiA has at least one clock-related activity: it stimulates KaiC autophosphorylation, which is functionally important for circadian timekeeping (7, 8). Data supporting this activity are also

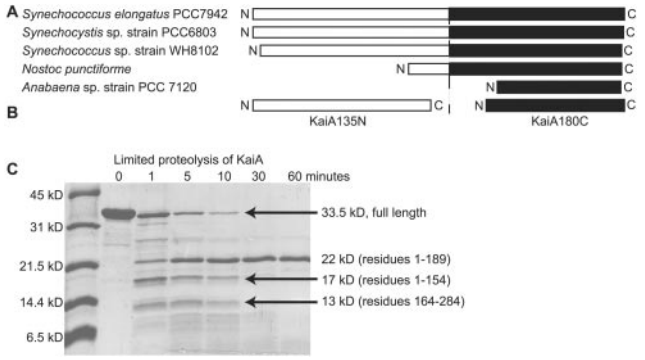

Fig. 2. (*A*) Graphic representation of five apparent KaiA homologs from the listed cyanobacteria. The amino termini are regions of low sequence similarity and are represented by white boxes. The carboxyl termini are regions of high sequence similarity and are represented by black boxes. (*B*) Graphic representation of the two independent domains derived from *S. elongatus* KaiA in this study. (*C*) An SDS/PAGE gel containing samples from a limited trypsin digest assay (see *Materials and Methods*). As indicated, we observed three major species. Production of the KaiA135N and KaiA180C domains was, in part, based on the largest and smallest of the three species.

reported in an accompanying article (9). Furthermore, KaiB has a negative role in the assay only when KaiA is present (Fig. 1*A*).

Two-Domain Structure of KaiA Protein. Sequence alignment suggested at least two types of KaiA proteins: long and short. The long versions (from the unicellular species *S. elongatus*, *Synechocystis* sp. strain PCC 6803, and *Synechococcus* sp. strain WH8102) consist of ≈300 aminoacyl residues. There is limited sequence conservation in the amino-terminal 200 residues of these proteins but a high degree of conservation in the carboxyl-terminal 100 residues. The short versions (from the filamentous species *Anabaena* sp. strain PCC 7120 and *Nostoc punctiforme*) are essentially independent carboxyl-terminal domains (Fig. 2*A*). Thus, two distinct regions, possibly independent domains, seemed likely. Note that results from searches of the filamentous organisms' annotated genomes for sequences resembling the amino-terminal region of a long KaiA protein were negative.

Limited proteolysis assays of the 284-residue KaiA protein from *S. elongatus* supported our presumption of two independently folded domains (Fig. 2*C*). Amino-terminal sequencing identified three major protein species, with apparent molecular weights of 22 kDa (residues 1–189), 17 kDa (residues 1–154), and 13 kDa (residues 164–284) from our proteolysis assays (Fig. 2*C*). CD spectra of the KaiA180C domain, corresponding to residues 180–284, revealed primarily α-helical structure (see supporting information, which is published on the PNAS web site, www.pnas.org). In addition, an ^{15}N heteronuclear single quantum coherence (HSQC) spectrum showed chemical shift dispersion consistent with an α-helical protein (see supporting information). Thus, we consider the KaiA180C domain to be independently folded.

The ^{15}N-HSQC spectrum of the KaiA189N domain, corresponding to residues 1–189, indicated that this portion of KaiA also folds independently (see supporting information). However, this domain contains a significant number of conformationally flexible residues. A series of carboxyl-terminal truncations showed that the smallest well folded amino-terminal domain consists of residues 1–135 (KaiA135N) (12). A CD spectrum of KaiA189N revealed higher helical content than the corresponding spectrum from our derived KaiA135N domain (see supporting information). The *S. elongatus* KaiA protein thus appears to contain two domains, the amino and carboxyl regions, connected by a helical linker of ≈50 residues (Fig. 2*B*).

***In Vitro* Function of Isolated KaiA Domains.** To address function we examined the rate of KaiC autophosphorylation in the presence of these two independent KaiA domains. Again, initial rate conditions were established for these assays. Addition of KaiA180C to the autophosphorylation assay described above gave results similar to full-length KaiA (Fig. 1*B*). Specifically, the rates of increase in KaiC autophosphorylation (≈2-fold), and net decrease on addition of KaiB were nearly identical in the presence of either KaiA protein or the KaiA180C domain (Fig. 1*B*). Addition of KaiA135N to the autophosphorylation assays produced no observable rate changes with or without KaiB protein (Fig. 1*C*). Thus, the domain of KaiA most highly conserved among the cyanobacteria, the carboxyl terminus, interacts with KaiC and stimulates autophosphorylation. The other KaiA domain, represented by KaiA135N and having much less sequence conservation, does not functionally interact with KaiC in this assay. However, we recognize that this domain is vitally important for generating circadian rhythmicity, based on phenotypic data from a large number of mutant *kaiA* alleles that encode point mutations manifest in the amino-terminal domain. Strains harboring these alleles have lengthened circadian periods in their gene expression rhythms (25).

Solution Structure of KaiA135N. The solution structure of KaiA135N provided insight into its function and, subsequently, into modeling KaiA protein function (Fig. 3 and supporting information). We used the Dali similarity search to compare KaiA135N structure with known protein structures (26). The six most similar structures, using the average minimized KaiA135N domain structure (Fig. 3*Ai*) as query, were all two-component-type receiver domains, namely, those from the DrrD, CheY, NarL, FixJ, Etr1, and AmiR proteins (27). This result was not anticipated by either sequence alignment or fold recognition algorithms (28). The average C^{α} rms deviation for these six receiver domains was 2.5 Å for 86% of the main chain, and the average structure similarity score (*Z* score) was 12.6. By comparison, a similarity search based on CheY protein (PDB ID 1JBE; ref. 29), the prototypical bacterial receiver domain, returned an average C^{α} rms deviation of 2.2 Å for 92% of the main chain with an average *Z* score of 15.5 for the best six receiver domain matches (*Z* score threshold for structurally similar proteins is 2; see supporting information). Conspicuously, KaiA135N lacks the conserved aspartyl residues necessary for the Mg^{+2}-dependent phosphoryl-transfer activity that defines canonical receiver domains (30). Direct comparison to CheY shows that Asp-57, Asp-12 and Asp-13 are transposed to Asn-60, Glu-12 and Ser-13 in the KaiA135N domain. Moreover, KaiA135N fails to bind Mg^{+2}, as titration with $MgCl_2$ did not show significant changes in the ^{15}N-HSQC spectrum (data not shown).

Effect of Residue Substitution on KaiA135N Structure. A number of *kaiA* alleles alter the periodicity of clock-regulated gene expression rhythms in *S. elongatus* (25, 31). Thirteen of these alleles encode amino acyl residue substitutions that lie within the KaiA135N domain. We produced each substituted domain and then examined the effects of residue substitution on KaiA135N structure by comparing their ^{15}N-HSQC spectra to that of the wild type under the same conditions. Five substitutions (L31P: prolyl for leucyl residue at position 31, S36P, C53S, V76G, and E103K) resulted in unfolded domains as judged by a lack of chemical shift dispersion in their spectra (data not shown). These domains also had decreased solubility compared with the wild type, based on their tendency to aggregate on concentration. One substitution (V76A) also tended to aggregate on concentration but its spectra showed better chemical shift dispersion than the others. All six of these substitutions involve buried residues and most likely perturb stabilizing interactions. The

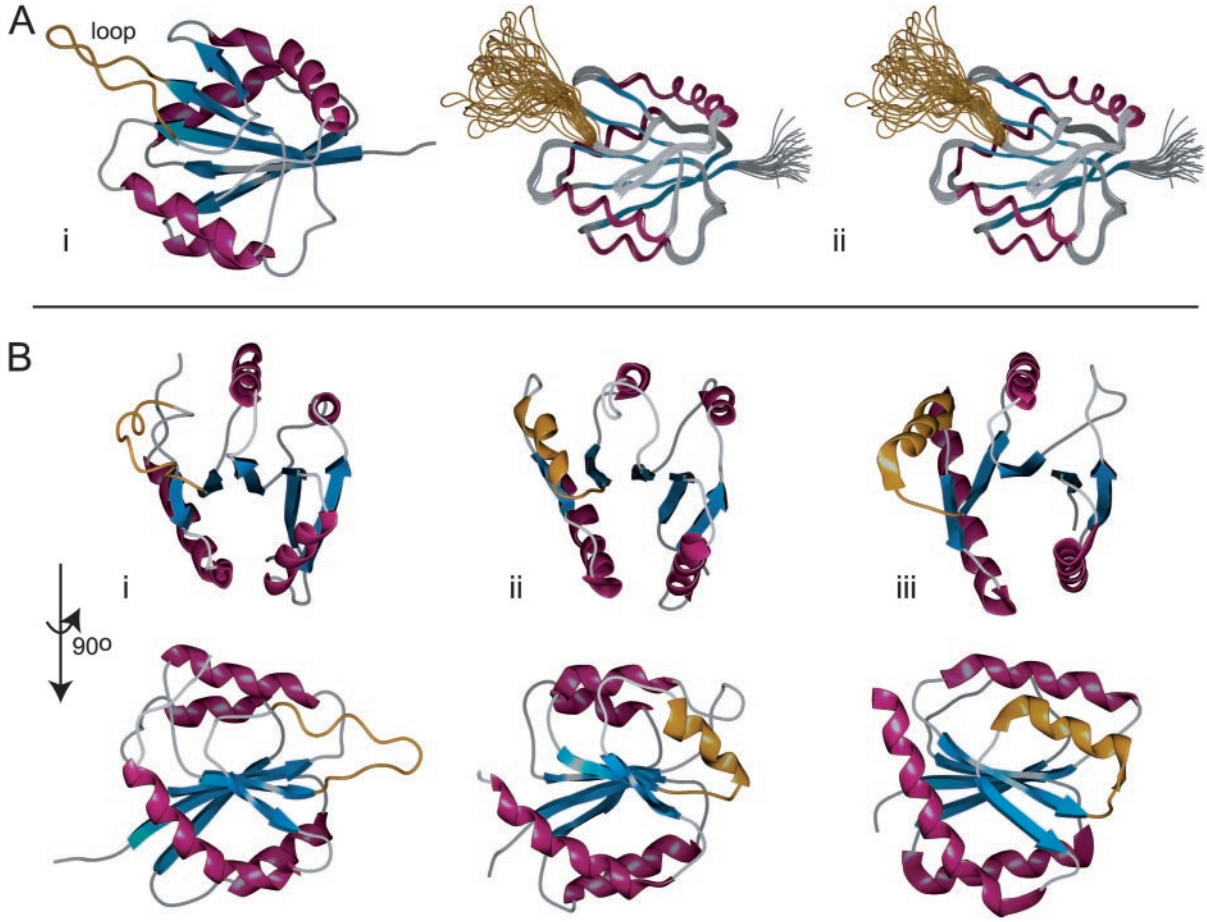

Fig. 3. The solution structure of KaiA135N and comparisons to other receiver domain proteins. β-strands are in blue, α-helices are in purple, and the flexible loop of KaiA135N and the equivalent region of other receiver domains are in gold. The structure coordinates have been deposited in the Protein Data Bank under PDB ID codes 1M2E and 1M2F for the average minimized structure and the family of structures, respectively. (*Ai*) Schematic representation of the average minimized structure. The solution structure of KaiA135N is an α-β-α sandwich built around a five-parallel-strand β-sheet with b-a-c-d-e arrangement. The rotational correlation time (τ_c) was calculated to be $\approx$8.2 ns, which is consistent with a monomer in solution (21). (*Aii*) Stereoview of the overlaid backbone of a family of 25 low-energy structures calculated from 2,034 distance and geometry restraints. The backbone rms deviation from the average is 0.38 $\pm$ 0.04 Å for residues 4–83 and 98–135. The rms deviation for all heavy atoms is 0.78 $\pm$ 0.05 Å for the same residues. Few medium- or long-range NOE contacts were identified for residues 83–97, and ^{15}N dynamics (see supporting information) showed that this region is highly dynamic. (*B*) Structural comparison of KaiA135N with other receiver domains. Shown here are KaiA135N (*Bi*), the NtrC (1DC7) receiver domain (*Bii*), and the AmiR (1QO0, residues 11–131) receiver domain (*Biii*) at two mutually orthogonal views. Figures were prepared with SPOCK (38).

remaining substitutions (I9T, I16F, Q113R, Q117L, D119E, D119G, V131A) gave stable KaiA135N domains whose ^{15}N-HSQC spectra were similar to that of the wild type. Five of these latter substitutions were in α2 or α4 and chemical shift comparison of each substituted domain's spectrum to that of the wild type revealed structural changes localized to a small area of the protein (Fig. 4).

Discussion

Despite the explicit structural similarities, KaiA135N should not be competent to function as a canonical receiver domain. It lacks the conserved aspartyl residues necessary for a Mg^{+2}-dependent phosphoryl-transfer activity. Instead, we propose that it is a pseudo-receiver domain and functions much like the corresponding domain in AmiR (Fig. 3*Biii*). Free AmiR protein activates aliphatic amidase operon expression in *Pseudomonas aeruginosa* via a transcription antitermination activity (32). However, in the absence of aliphatic amides, AmiC protein binds directly to the AmiR pseudo-receiver domain and effectively sequesters AmiR. This action allows transcription termination of the amidase operon message. Interestingly, the AmiR protein's binding interface is α4 (32). The corresponding α-helix in CheY is the interface between that protein and its cognate, signal transducing, protein kinase CheA (33). Furthermore, receiver domain α4 helices are flexible and this flexibility evidently allows switching between inactive and active states (34). These states then regulate other regions/activities of the respective proteins (34–36). In the KaiA135N domain however, this interface-helix is replaced by an unstructured, solvent-exposed loop composed of residues 83–97 (Fig. 3*Ai*) as shown both by the almost complete lack of medium or long-range ^{1}H–^{1}H NOEs and ^{15}N backbone dynamics analysis (see supporting information). This loop may serve a similar interfacing role for the KaiA protein. However, consideration of a set of seven amino acyl residue substitutions in the KaiA135N domain, which alter the periodicity of clock-regulated gene expression rhythms (25, 31), yet result in folded, stable proteins, suggests another KaiA protein interface. The period-altering substitutions I16F, Q113R, Q117L, D119E, and D119G, map on α2 or α4 and cause only localized changes in the protein (Fig. 4); therefore, we also consider this part of the KaiA135N domain as a potential protein-interacting surface. It will be interesting to determine

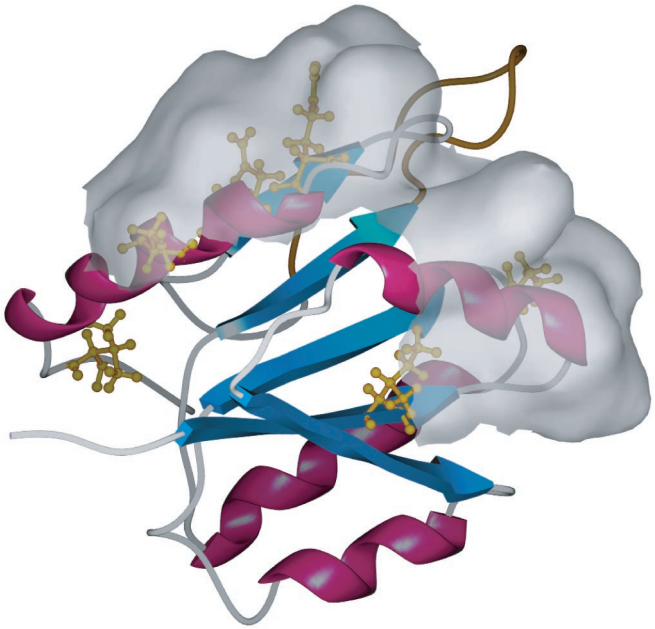

Fig. 4. Stable KaiA135N clock-period altering mutations and a putative protein-interacting surface. Shown here is the average minimized structure of KaiA135N. Residue substitutions that yield stable proteins *in vitro* are shown in gold. Most of these residues are mapped on α2 or α4 (I16F, Q113R, Q117L, D119E, D119G). Chemical shift analysis of the mutant proteins versus the wild-type protein showed changes extending over these two helices. Shown here is the water-accessible surface of the residues affected by these mutations. We postulate that this surface is important for signal transduction either between KaiA135N and an upstream signal component or between the two KaiA domains.

whether this surface and the unstructured, solvent-exposed loop are important for interactions with an upstream signal-input protein, or for KaiA interdomain communication.

A pseudo-receiver domain is also found in two other circadian clock proteins, TOC1 from *A. thaliana* and CikA from *S. elongatus* (10, 37). Thus, a second potential evolutionary connection between plant and cyanobacterial circadian timekeeping mechanisms has been identified. The *cikA* gene in *S. elongatus* encodes a bacteriophytochrome, and phytochromes are integral components of plant circadian rhythm generation (11). Conceivably, these two *S. elongatus* circadian clock components have a functional connection. If, as we have argued, KaiA receives environmental cues via its pseudo-receiver domain, then some of those cues likely originate from the environmentally responsive, phase-resetting CikA protein. We have also demonstrated a likely activity for those cues to ultimately influence: modulation by KaiA of the rate at which KaiC autophosphorylates.

Consequently, we model timekeeping as changes in the phosphorylation rate of KaiC protein (Fig. 5). The KaiC phosphorylation state may determine the protein's degradation rate as is true for eukaryotic clock proteins FRQ and PER (3); may influence other possible activities such as chromosome condensation (7); may determine its aggregation state in homo- and

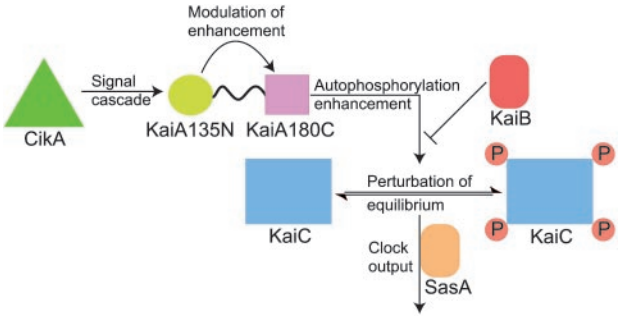

Fig. 5. Working model of KaiA protein function and its role in *S. elongatus* circadian timekeeping. CikA and other environmental sensors initiate signal transduction cascades that result in activation of the KaiA pseudo-receiver domain. This activation modulates the KaiA carboxyl-terminal domain's enhancement of the KaiC autophosphorylation rate. Thus, equilibria between KaiC phosphorylation states are perturbed. These states differentially control clock output, possibly through the SasA protein kinase. In this manner, a cycle of input, oscillation, and output can be established.

heterotypic interactions (5, 8); may alter its interaction with regulatory proteins such as the SasA protein kinase (10); or may affect aspects of all these potential activities. Although there are not yet sufficient data to distinguish among these functional possibilities, we favor a model that includes phosphorylation as a potential degradation signal for two reasons. First, ectopic overproduction of KaiA, expected to increase the rate of KaiC turnover, causes elevated (and arrhythmic) *kaiC* gene expression patterns (2). Second, ectopic overproduction of KaiC, expected to decrease the rate of KaiC turnover, represses (and makes arrhythmic) *kaiC* gene expression patterns (2). These data fit into a feedback regulatory mechanism as required for the cyclic patterns of gene expression harmonized by the circadian clock. Comparisons among cyanobacterial genomes would further suggest that stimulation of KaiC autophosphorylation by the carboxyl-terminal domain of KaiA is a conserved function. However, input signaling, as we propose for the *S. elongatus* KaiA amino-terminal domain, can be achieved by various mechanisms. This finding is not surprising given that sequence similar to that of *S. elongatus* ' CikA protein is also not ubiquitous among cyanobacteria (11). Variations in input mechanisms likely reflect the diversity of cyanobacterial metabolism and habitat.

We thank T. Kondo, H. Iwasaki, T. Nishiwaki, Y. Kitayama, and M. Nakajima (Nagoya University, Nagoya, Japan) for sharing unpublished results. We also thank P. LiWang for assistance and helpful discussions, Michael Polymenis for insight, and K. Koshlap for NMR support. J. Ditty and S. Canales improved the manuscript. We thank Larry Dangott and the Protein Chemistry Lab for amino terminal sequencing. NMR instrumentation at Texas A&M University is supported by National Science Foundation Grant DBI-9970232 and by the Texas Agricultural Experiment Station. Financial support was provided by National Institutes of Health Grant 1R01GM064576-01 (to A.C.L.), National Science Foundation Grant MCB-9982852 and the Texas Higher Education Coordinating Board Advanced Research Project 010366-0076-1999 (to S.S.G.), and National Institutes of Health National Research Science Award F32GM19644 (to S.B.W.).

1. Golden, S. S., Johnson, C. H. & Kondo, T. (1998) *Curr. Opin. Microbiol*. **1,** 669–673.
2. Ishiura, M., Kutsuna, S., Aoki, S., Iwasaki, H., Andersson, C. R., Tanabe, A., Golden, S. S., Johnson, C. H. & Kondo, T. (1998) *Science* **281,** 1519–1523.
3. Young, M. W. & Kay, S. A. (2001) *Nat. Rev. Genet*. **2,** 702–715.
4. Lorne, J., Scheffer, J., Lee, A., Painter, M. & Miao, V. P. (2000) *FEMS Microbiol. Lett*. **189,** 129–133.
5. Iwasaki, H., Taniguchi, Y., Ishiura, M. & Kondo, T. (1999) *EMBO J.* **18,** 1137–1145.
6. Xu, Y., Mori, T. & Johnson, C. H. (2000) *EMBO J.* **19,** 3349–3357.
7. Mori, T. & Johnson, C. H. (2001) *Semin. Cell Dev. Biol.* **12,** 271–278.
8. Nishiwaki, T., Iwasaki, H., Ishiura, M. & Kondo, T. (2000) *Proc. Natl. Acad. Sci. USA* **97,** 495–499.
9. Iwasaki, H., Nishiwaki, T., Kitayama, Y., Nakajima, M. & Kondo, T. (2002) *Proc. Natl. Acad. Sci. USA* **99,** 15788–15793.
10. Iwasaki, H., Williams, S. B., Kitayama, Y., Ishiura, M., Golden, S. S. & Kondo, T. (2000) *Cell* **101,** 223–233.
11. Schmitz, O., Katayama, M., Williams, S. B., Kondo, T. & Golden, S. S. (2000) *Science* **289,** 765–768.

12. Vakonakis, I., Risinger, A. T., Latham, M. P., Williams, S. B., Golden, S. S. & LiWang, A. C. (2001) *J. Biomol. NMR* **21,** 179–180.
13. Wüthrich, K. (1986) *NMR of Proteins and Nucleic Acids* (Wiley, New York).
14. Madsen, J. C., Sorensen, O. W., Sorensen, P. & Poulsen, F. M. (1993) *J. Biomol. NMR* **3,** 239–244.
15. Grzesiek, S., Kuboniwa, H., Hinck, A. P. & Bax, A. (1995) *J. Am. Chem. Soc.* **117,** 5312–5315.
16. Grzesiek, S. & Bax, A. (1993) *J. Biomol. NMR* **3,** 185–204.
17. Vuister, G. W., LiWang, A. C. & Bax, A. (1993) *J. Am. Chem. Soc.* **115,** 5334–5335.
18. Bax, A., Max, D. & Zax, D. (1992) *J. Am. Chem. Soc.* **114,** 6924–6925.
19. Cornilescu, G., Delaglio, F. & Bax, A. (1999) *J. Biomol. NMR* **13,** 289–302.
20. Clore, G. M. & Gronenborn, A. M. (1991) *Science* **252,** 1390–1399.
21. LiWang, A. C., Cao, J. J., Zheng, H., Lu, Z., Peiper, S. C. & LiWang, P. J. (1999) *Biochemistry* **38,** 442–453.
22. Bronger, A. T. (1987) X-PLOR: A System for X-Ray Crystallography and NMR (Yale University Press, New Haven, CT), Version 3.1.
23. Kuszewski, J., Gronenborn, A. M. & Clore, G. M. (1996) *Protein Sci*. **5,** 1067–1080.
24. Kuszewski, J., Gronenborn, A. M. & Clore, G. M. (1997) *J. Magn. Reson*. **125,** 171–177.
25. Nishimura, H., Nakahira, Y., Imai, A., Tsuruhara, A., Kondo, H., Hayashi, H., Hirai, M., Saito, H. & Kondo, T. (2002) *Microbiology* **148,** 2903–2909.
26. Holm, L. & Sander, C. (1998) *Nucleic Acids Res.* **26,** 316–319.
27. Volz, K. (1993) *Biochemistry* **32,** 11741–11753.
28. Kelley, L. A., MacCallum, R. M. & Sternberg, M. J. (2000) *J. Mol. Biol.* **299,** 499–520.
29. Simonovic, M. & Volz, K. (2001) *J. Biol. Chem.* **276,** 28637–28640.
30. Bourret, R. B., Hess, J. F. & Simon, M. I. (1990) *Proc. Natl. Acad. Sci. USA* **87,** 41–45.
31. Kondo, T. & Ishiura, M. (1994) *J. Bacteriol*. **176,** 1881–1885.
32. O'Hara, B. P., Norman, R. A., Wan, P. T., Roe, S. M., Barrett, T. E., Drew, R. E. & Pearl, L. H. (1999) *EMBO J.* **18,** 5175–5186.
33. Welch, M., Chinardet, N., Mourey, L., Birck, C. & Samama, J. P. (1998) *Nat. Struct. Biol* **5,** 25–29.
34. Volkman, B. F., Lipson, D., Wemmer, D. E. & Kern, D. (2001) *Science* **291,** 2429–2433.
35. Hwang, I., Thorgeirsson, T., Lee, J., Kustu, S. & Shin, Y. K. (1999) *Proc. Natl. Acad. Sci. USA* **96,** 4880–4885.
36. Kern, D., Volkman, B. F., Luginbuhl, P., Nohaile, M. J., Kustu, S. & Wemmer, D. E. (1999) *Nature* **402,** 894–898.
37. Strayer, C., Oyama, T., Schultz, T. F., Raman, R., Somers, D. E., Más, P., Panda, S., Kreps, J. A. & Kay, S. A. (2000) *Science* **289,** 768–771.
38. Christopher, J. (1999) SPOCK: The Structural Properties Observation and Calculation Kit (Center for Macromolecular Design, Texas A&M University, College Station, TX).